Abstracts

CATALYSIS – APPLIED AND PHYSICAL ASPECTS

Microbial Engineering of Nanoheterostructures: Biological Synthesis of a Magnetically Recoverable Palladium Nanocatalyst

V. S. Coker, J. A. Bennett, N. D. Telling, T. Henkel, J. M. Charnock, G. van der Laan, R. A. D. Pattrick, C. I. Pearce, R. S. Cutting, I. J. Shannon, J. Wood, E. Arenholz, I. C. Lyon and J. R. Lloyd, *ACS Nano*, 2010, **4**, (5), 2577–2584

Pd nanoparticles were deposited onto a nanoscale biogenic magnetite support without the need for pre-treatment with a ligand. The support was synthesised in a one-step process at ambient temperature by the Fe(III)-reducing bacterium, *Geobacter sulfurreducens*. The resulting Pd-magnetite catalyst showed ease of recovery and high dispersion. Rates of reaction for Heck coupling of iodobenzene to ethyl acrylate or styrene were equal or superior to a commercial colloidal Pd catalyst.

Banana Peel Extract Mediated Novel Route for the Synthesis of Palladium Nanoparticles

A. Bankar, B. Joshi, A. R. Kumar and S. Zinjarde, *Mater. Lett.*, 2010, **64**, (18), 1951–1953

Pd nanoparticles with average size 50 nm were synthesised in a 'green' process by reducing $PdCl_2$ using boiled, crushed, acetone precipitated, air-dried banana peel powder. The Pd nanoparticles were characterised by UV–vis spectroscopy, SEM-EDS, XRD analysis, DLS and FTIR spectroscopy.

Solid-State NMR Characterization of Wilkinson's Catalyst Immobilized in Mesoporous SBA-3 Silica

A. Grünberg, X. Yeping, H. Breitzke and G. Buntkowsky, *Chem. Eur. J.*, 2010, **16**, (23), 6993–6998

Wilkinson's catalyst [$RhCl(PPh_3)_3$] was immobilised inside the pores of amine functionalised mesoporous silica material SBA-3. Successful modification of the silica surface was confirmed by ^{29}Si CP-MAS NMR experiments. ^{31}P-^{31}P *J*-resolved 2D MAS NMR experiments were used to characterise the binding mode of the immobilised catalyst. Two PPh_3 ligands were found to be replaced and the catalyst was bonded to the silica surface through the amine groups of two linker molecules attached to the silica surface.

Gaseous Fuel Production from Nonrecyclable Paper Wastes by Using Supported Metal Catalysts in High-Temperature Liquid Water

A. Yamaguchi, N. Hiyoshi, O. Sato, K. K. Bando and M. Shirai, *ChemSusChem*, 2010, **3**, (6), 737–741

Gasification of nonrecyclable paper wastes, such as shredded documents and paper sludge, was carried out in high-temperature liquid water over supported Ru, Rh, Pt or Pd catalysts to produce CH_4 and CO_2, with a small amount of H_2. The order of catalytic activity was Ru > Rh >> Pt >> Pd. The most effective catalyst was Ru/C. Paper wastes were gasified to a limited degree (32.6 C%) for 30 min in water at 523 K. At 573 K, more complete gasification with almost 100 C% was achieved within 10 min.

CATALYSIS – INDUSTRIAL PROCESS

Investigation of the Catalytic Activity of Rh–$LaCoO_3$ Catalyst in the Conversion of Tar from Biomass Devolatilization Products

P. Ammendola, R. Chirone, L. Lisi, B. Piriou and G. Russo, *Appl. Catal. A: Gen.*, 2010, **385**, (1–2), 123–129

An alumina-supported Rh–$LaCoO_3$ catalyst can be used to convert biomass devolatilisation products to syngas in a double fixed bed reactor system. The reaction was tested at temperatures 500–700°C, Rh loadings 0.1–1 wt%, catalyst amount 0.25–1 g and N_2 flow rate 12–60 Nl h^{-1}. Good performance was achieved at 600°C. At 700°C complete tar conversion could be obtained with a Rh loading of 0.1 wt%, a catalyst amount of 0.5 g or a carrier flow rate of 48 Nl h^{-1}.

CATALYSIS – REACTIONS

Rapid Identification of a Scalable Catalyst for the Asymmetric Hydrogenation of a Sterically Demanding Aryl Enamide

L. Lefort, J. A. F. Boogers, T. Kuilman, R. J. Vijn, J. Janssen, H. Straatman, J. G. de Vries and A. H. M. de Vries, *Org. Process Res. Dev.*, 2010, **14**, (3), 568–573

High-throughput screening was used to find a cost-effective and scalable Rh-based catalyst with a bulky monodentate phosphite ligand for the asymmetric hydrogenation of a sterically demanding enamide as an intermediate towards a new potent melanocortin receptor agonist useful in the treatment of obesity.

© 2010 Johnson Matthey

The catalyst was scaled up and used in the kilogram production of the desired bulky chiral amide.

Enhanced Bulk Catalyst Dissolution for Self-Healing Materials

T. C. Mauldin and M. R. Kessler, *J. Mater. Chem.*, 2010, **20**, (20), 4198–4206

A model was developed to aid in the selection of healing monomers that can rapidly dissolve catalysts in self-healing materials. Predictions were made of dissolution rates of Grubbs' catalyst [$Cl_2(PCy_3)_2Ru(=CHPh)$] in a small library of ROMP-active norbornenyl-based healing monomers. It was observed that healing monomers and blends of monomers with Hansen parameters similar to the catalyst were able to rapidly dissolve the catalyst. Increasing the dissolution rate of the catalyst allows less overall catalyst to achieve similar levels of healing, making Grubbs' catalyst potentially more economic for use.

EMISSIONS CONTROL

In Situ Synthesis of Platinum Nanocatalysts on a Microstructured Paperlike Matrix for the Catalytic Purification of Exhaust Gases

H. Koga, Y. Umemura, A. Tomoda, R. Suzuki and T. Kitaoka, *ChemSusChem*, 2010, **3**, (5), 604–608

Pt nanoparticles (PtNPs) on a microstructured paperlike matrix of ceramic fibre and zinc oxide whiskers (PtNPs@ZnO "paper") were synthesised *in situ*. Good catalytic performance was demonstrated for the reduction of NOx with propene for exhaust gas purification, at a low reaction temperature and with one-third the dosage of Pt compared to conventional Pt-loaded honeycomb catalysts.

Sulfur Release from a Model Pt/Al_2O_3 Diesel Oxidation Catalyst: Temperature-Programmed and Step-Response Techniques Characterization

J.-Y. Luo, D. Kisinger, A. Abedi and W. S. Epling, *Appl. Catal. A: Gen.*, 2010, **383**, (1–2), 182–191

The desulfation process of a model Pt/Al_2O_3 DOC was investigated using temperature-programmed techniques and step-response methods. Desulfation was promoted under reducing conditions. H_2O further promoted desulfation while CO_2 had no obvious effect. Higher H_2 concentrations generated more H_2S. The desulfation process could be viewed as a stepwise reduction of sulfates to SO_2 and then to H_2S. A S loading equivalent to 3 g l^{-1} gave the largest SO_2:H_2S ratio.

METALLURGY AND MATERIALS

Atomic-Level Pd–Pt Alloying and Largely Enhanced Hydrogen-Storage Capacity in Bimetallic Nanoparticles Reconstructed from Core/Shell Structure by a Process of Hydrogen Absorption/Desorption

H. Kobayashi, M. Yamauchi, H. Kitagawa, Y. Kubota, K. Kato and M. Takata, *J. Am. Chem. Soc.*, 2010, **132**, (16), 5576–5577

Solid-solution homogeneous PdPt nanoparticles, **1**, containing ~21 at% Pt were formed from core/shell nanoparticles with a Pd core of diameter 6.1 ± 0.1 nm and a Pt shell of thickness ~1.1 nm by a process of H_2 absorption/desorption at 373 K. No size growth was observed during the process. **1** had a higher H_2-storage capacity than Pd nanoparticles and this could be tuned by changing the alloy composition.

Microstructure and Corrosion of Pd-Modified Ti Alloys Produced by Powder Metallurgy

M. A. Ashworth, A. J. Davenport, R. M. Ward and H. G. C. Hamilton, *Corros. Sci.*, 2010, **52**, (7), 2413–2421

Ti alloy parts with enhanced corrosion resistance were fabricated by a powder metallurgy route. Commercial purity Ti powders were modified with 0.15 wt% Pd and hot isostatically pressed (HIPped). The microstructure and distribution of the Pd was characterised by optical microscopy and SEM. The phase composition and electrochemistry of the HIPped Pd-modified alloy was equivalent to that of wrought Grade 7 Ti (which contains 0.12–0.25 wt% Pd). This route overcomes the need to source and maintain an inventory of expensive Pd-modified grades of Ti and allows "on-demand" modification of powders with the level of Pd tailored towards the target application.

APPARATUS AND TECHNIQUE

Inactivation and Mineralization of Aerosol Deposited Model Pathogenic Microorganisms over TiO_2 and Pt/TiO_2

E. A. Kozlova, A. S. Safatov, S. A. Kiselev, V. Yu. Marchenko, A. A. Sergeev, M. O. Skarnovich, E. K. Emelyanova, M. A. Smetannikova, G. A. Buryak and A. V. Vorontsov, *Environ. Sci. Technol.*, 2010, **44**, (13), 5121–5126

Air disinfection from bacteria and viruses was carried out on undoped TiO_2 and on platinised sulfated TiO_2 (Pt/TiO_2) under UVA irradiation and in the dark. ~90% inactivation was achieved after 30 min irradiation on TiO_2 and 90–99.8% on Pt/TiO_2. The rate of photocatalytic CO_2 production increased with both cell mass

© 2010 Johnson Matthey

increase and photocatalyst mass increase. Pt/TiO_2 showed higher rates of mineralisation and inactivation of microorganisms, likely due to a better charge carrier separation.

ELECTRICAL AND ELECTRONICS

Nonvolatile Metal–Oxide–Semiconductor Capacitors with Ru-RuO_x Composite Nanodots Embedded in Atomic-Layer-Deposited Al_2O_3 Films

H.-Y. Gou, S.-J. Ding, Y. Huang, Q.-Q. Sun, W. Zhang, P.-F. Wang and Z. Chen, *J. Electron. Mater.*, 2010, **39**, (8), 1343–1350

Ru-RuO_x composite nanodots ('RONs') were grown on atomic-layer-deposited Al_2O_3 films using magnetic sputtering of a Ru target followed by postdeposition annealing. 'RONs' with density ~2 × 10^{12} cm^{-2} were obtained with good uniformity. Metal–oxide–semiconductor capacitors with 'RONs' embedded in Al_2O_3 films were electrically characterised for different configurations of tunnelling layers (T)/blocking layers (B), and the underlying mechanisms of charge storage were studied. For a 6 nm T/22 nm B device, a memory window of 3.7 V was achieved for a ±7 V programming/erasing voltage for 0.1 ms, with charge retention of more than 80% after 10 years.

MEDICAL AND DENTAL

Osmium(II)– *versus* Ruthenium(II)–Arene Carbohydrate-Based Anticancer Compounds: Similarities and Differences

M. Hanif, A. A. Nazarov, C. G. Hartinger, W. Kandioller, M. A. Jakupec, V. B. Arion, P. J. Dyson and B. K. Keppler, *Dalton Trans.*, 2010, **39**, (31), 7345–7352

Os(II)–arene complexes with carbohydrate-derived phosphite co-ligands were synthesised and their *in vitro* anticancer activity assessed. The Os compounds exhibited slightly higher IC_{50} values than analogous Ru(II)–arene complexes, however the rate of hydrolysis was very slow. Within the series of Os compounds, *in vitro* anticancer activity was highest for the most lipophilic chlorido complex.

NANOTECHNOLOGY

Shape-Controlled Synthesis of Single-Crystalline Palladium Nanocrystals

W. Niu, L. Zhang and G. Xu, *ACS Nano*, 2010, **4**, (4), 1987–1996

Single-crystalline rhombic dodecahedral, cubic and octahedral Pd nanocrystals (see the Figure below) and their derivatives were selectively synthesised with varying degrees of edge- and corner-truncation by a seed-mediated method. $(C_{16}H_{33})N(CH_3)_3Br$ was used as surfactant, KI as additive and ascorbic acid as reductant. At constant ascorbic acid concentration, Pd nanocrystal shapes were affected by concentration of KI and reaction temperature. At zero, very low or relatively high KI concentrations, the {100} Pd facets were favoured. At medium KI concentration, the {110} Pd facets were favoured at high temperatures and the {111} Pd facets at low temperatures. These results provide mechanistic insights into the growth of well-faceted Pd nanostructures for applications such as H_2 storage, gas sensing and catalysis.

W. Niu *et al.*, *ACS Nano*, 2010, **4**, (4), 1987–1996

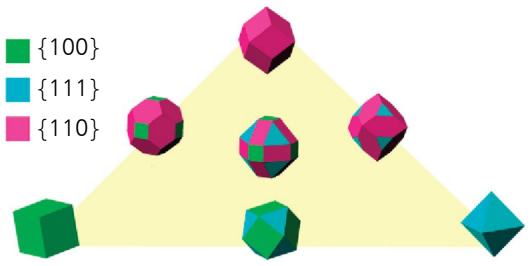

Image reproduced with permission from *ACS Nano*. Copyright 2010 American Chemical Society

SURFACE COATINGS

Atomic Layer Deposition of Ir–Pt Alloy Films

S. T. Christensen and J. W. Elam, *Chem. Mater.*, 2010, **22**, (8), 2517–2525

Atomic layer deposition (ALD) was used to prepare thin-film mixtures of Ir and Pt. By controlling the ratio between the Ir(III) acetylacetonate/O_2 cycles for Ir ALD and the (trimethyl)methylcyclopentadienyl Pt(IV)/O_2 cycles for Pt ALD, the Ir/Pt ratio in the films could be controlled precisely. Nucleation and growth of each metal proceeded smoothly, with negligible perturbation caused by the presence of the other metal, so that the composition and growth per cycle followed rule-of-mixtures formulae. ALD may be a facile and general approach for preparing noble metal alloy films and nanostructures for catalysis, chemical sensors, microelectronics, corrosion resistance, medicine, and other fields.

 © 2010 Johnson Matthey